Available online at www.CivileJournal.org

Civil Engineering Journal

Vol. 5, No. 5, May, 2019

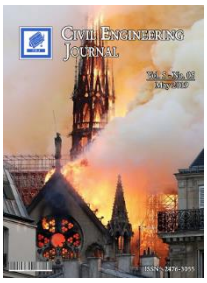

Experimental Investigation for Effects of Mini-piles on the Structural Response of Raft Foundations

Huda Hussein Ahmed [a*], Salah Rohaima Al-Zaidee [b]

[a] *M. Sc. Student, College of Engineering-University of Baghdad, Baghdad, Iraq.*

[b] *Assistant Professor, College of Engineering-University of Baghdad, Baghdad, Iraq.*

Received 13 March 2019; Accepted 9 May 2019

Abstract

Mini-piles made their debut as a cost-effective way to stabilize the historical structures. Recently, mini-piles have increased in popularity all over the world and are being used for bridges, buildings, slope stability, antenna towers, and residential construction. This paper presents the preparing, executing, data acquisition, and result presentation for an experimental work concerns with five scale-down mini-piled raft foundation models. All models were prepared to study the effectiveness of the mini-piled raft foundation in reducing the settlement and the bending moments. Five tests have been achieved. The reference first test includes a raft foundation with 15mm thickness. Second, third, and fourth tests are mini-piled raft foundations with five mini-piles and with thicknesses of 15 mm, 10 mm, and 8mm respectively. Finally, the fifth test dealt with a single mini-pile 178mm in length and 6mm in diameter. It has been adopted to investigate the reference behavior of the single mini-pile. When they were used, the piles have 42 mm center to center distances. A scale-down factor of $1/45$, a sandy soil with with ϕ of 40^o, and relative density of 60% have been considered in all tests. Test results indicated a 45% decrease in settlement for 15mm mini-piled raft foundation comparing with the reference 15mm raft foundation. Moreover, there is no significant difference in settlement between 15mm mini-piled raft foundation comparing with the 10mm and 8mm thick mini-piled raft foundations. Regarding to the bending moments, they decrease at the mid and edge of the 15mm mini-piled raft foundation comparing to those of the reference raft foundation. It has also been noted that the moments are inversely proportional to the thickness of the piled raft foundations. With respect to the mini-piles, it has been found that most of the pile axial loads are transferred to the underneath soil through friction and this friction increases as the raft thickness decreases.

Keywords: Mini-Pile; Raft Foundation; Sandy Soil; Settlement; Bending Moment; Friction.

1. Introduction

A mini-pile is a drilled pile with a diameter equivalent to or less than 300 mm and lengths up to 30 m. It is having a small diameter to length ratio so that it is slender in nature, most of the load is transferred to the soil by friction FHWA (2005) [1]. Mini-piles construct in Europe at the beginning to retrofit the historic and the sensitive structures that had damage during World War II. As the development of geomechanics, a need for mini-piles was increased. Mini-pile technology is predicted to begin in Italy during the 1950 by Fernando Lizzi, and it was seen in the United States in the 1980 Bruce (1997) [2].

Since then, much collaboration and research has been done in the area of mini-pile design and construction. Today, mini-piles are effectively utilized in various scenarios including building underpinning, excavation stabilization, and

* Corresponding author: eng.huad81@gimal.com

http://dx.doi.org/10.28991/cej-2019-03091313

slope stability. A growing understanding of soil mechanics and the seismic effects on foundations has given rise to the use of mini-piles. Deteriorating and ageing buildings require foundation retrofitting to resist the continuing loads from the environment and structure. The versatility of mini-pile construction has allowed effective stabilization of many older structures Barron (2016) [3].

There are many studies have been lead to evaluate the performance of mini-pile in sandy soil under various types of loading. Different techniques for testing have been employed such as full-scale mini-pile load tests, $1g$ physical modeling, and the centrifuge modeling. Jeon & Kulhawy (2001) presents a full-scale field tests on 21 mini-piles with different diameters and lengths, eight mini-piles were installed in clay soils and thirteen in sandy soils. The results of the test indicate that the mini-pile load carrying capacity per pile volume can be higher than larger diameter drilled shafts for shaft depth to diameter ratio less than 100. This increase is about 1.5 to 2.5 for mini-piles installed in sandy soil [4].

Tsukada et al. (2006) evaluated the improvement in bearing capacity of spread footings reinforced with mini-piles in sandy soil has different densities by using small models. They found that the bearing capacity of the foundations increased in dense sand [5]. Kyung et al. (2016) presented an experimental testing program on a series of model load tests to investigate the vertical load-carrying behavior of mini-piles for various parametric such as installation angle, pile spacing, and foundation type applicable for mini-piles [6]. Tae (2017) investigated the characteristics of a mini-piled raft through model tests and a numerical analysis. The behavior of the mini-piled raft is evaluated for various conditions, such as soil type, pile length, and installation angle [7]. Sharma et al. (2019) studied the behavior of an experimental model for group mini-piles in sand. In this study three important parameters, length to diameter ratio (L/D), spacing of piles and relative density of sand were considered. Efficiency of the groups increases with the increase in L/D ratio at 30% and 50% relative density but it is opposite at 80% relative density [8]. Geotechnical centrifuge testing was conducted by Alnuaim et al (2015) in order to investigate the behavior of mini-piled raft foundations with different raft thickness in sandy soil and evaluate their performance characteristics [9].

Several authors have been presented results of numerical simulations for settlement reducing piles, Rose et al. (2013) [10] Investigated the performance of micro pile groups in clays using geotechnical centrifuge testing and numerical modeling. Alnuaim et al. (2016) presented a numerical investigation on the performance of micro piled raft foundation in sand. Calibrated and verified finite element model with centrifuge tests [11]. Zolfegharifar et al. (2015) Presents analyze the group function of mini-piles with different length and numbers on a two-layer soil bed with using the Abaqus software and three dimensional modeling [12]. El Sharnouby (2018) investigated through three-dimensional finite-element analysis the axial compression behavior of reinforced helical pull-down micro piles and fiber-reinforced polymer. The model was calibrated using the results of full-scale load tests conducted by the authors [13].

A number of studies have been evaluated the piled raft foundation performance such as Poulos & Davis (1974) [14]), Randolph (1994) [15], Poulos (2001) [16], Tuna (2016) [17], and Ling-Yu Xu et al. [18] Mahboubi & Nazari-Mehr, (2010) evaluated the single and groups mini-pile performance in sandy soil under dynamic loading and using a finite element method to validate the results of centrifuge test [19]. In addition, several mini-pile tests were evaluated the lateral performance of mini-piles such as Richards & Rothbauer (2004) [20], Shahrour & Ata (2002) [21], Teerawut (2002) [22], and Kershaw & Luna (2018) a total of seventeen model micro piles were tested to investigate the effect of simultaneous axial and lateral loading on micro pile foundations, the results of the study indicated that the lateral deflection was only significantly affected by the introduction of a constant axial load for large lateral loads [23].

In addition to focus on the geotechnical aspect of the settlement reduction and how it is affected by the mini-piles, this study innovatively concerns with the structural aspect of how using mini-piles can reduce the bending moments in raft foundation.

2. Materials and Methods

Full-scale tests are the best approach to predict the behavior of mini-piles. To reduce the cost, time, and effort of the test, small-scale models are usually used in the laboratory instead of the full-scale tests. On the other hand, the scale-down models have great advantage as they permit a full control for the geotechnical properties of the soil and for the details of the model used in the tests. Boundary conditions and loading of the model can be specified, to explain in what technique that the loads are applied. In addition, small tank and quantity of the soil, small lengths of the mini-piles and raft, and small load are required to carry out the test compared with those requirements in prototype Wood (2004) [24].

In this study, the testing program consisted of the following tests: (1) one test on a single mini-pile; (2) one test on a raft with a thickness equivalent to 15 mm (3) three tests on five mini-piled group with different raft thicknesses of 8mm, 10mm and 15mm. All tests were performed on a dry sandy soil with a relative density, D_r, of 60%. All piles have a diameter of 6mm and a length of 178mm. Scale-down for all models has been determined based on Equation 1 and 2.

$$\frac{E_m A_m}{E_p A_p} = n_l^2 n_G \quad (1)$$

$$\frac{E_m I_m}{E_p I_p} = n_l^4 n_G \quad (2)$$

Where: $E_p A_p$ is the axial rigidity for the prototype element of the mini-pile.

$E_m A_m$ is the axial rigidity for the model element of the mini-pile.

$E_p I_p$ is the flexural rigidity for the prototype element of the raft.

$E_m I_m$ is the flexural rigidity for the model element of the raft.

n_l is scale factor for length ($n_l = 1/n$), and $n = 45$.

n_G is scale factor for shear stiffness, ($n_G = 1/n^{\alpha}$). Experimental experience suggests that the exponent α might be in the order of 0.5 for sands Wood (2004) [24].

In order to work with reasonable size, the model rafts and piles were fabricated using PVC with elastic modulus, E, of 2900 MPa and Poisson ratio, ν, of 0.4 (E=2900 MPa,ν= 0.4), which has a modulus of elasticity smaller than that of the prototype material, concrete. Table 1 shows the models and the corresponding prototypes dimensions along with the appropriate scaling laws:

Table 1. Scale factors

Description	Scaling law	Prototype (m)	Model (mm)
Mini-pile Diameter	$E_p\ A_p = n^{(2+\alpha)}$	0.20	6
Mini-pile Length	$1/n$	8.0	178
Raft Width	$1/n$	5.25	117
Raft Thickness	$E_p\ I_p = n^{(4+\alpha)}$	0.6	15
Raft Thickness	$E_p\ I_p = n^{(4+\alpha)}$	0.4	10
Raft Thickness	$E_p\ I_p = n^{(4+\alpha)}$	0.3	8

3. Test Setup

All model tests were conducted using the setup shown in Figure 1, which consists of a loading frame, loading jack, loading cell, piled-raft, and soil tank. The vertical load was applied to the models by means of 10-ton hydraulic compression handle jack. During all the experimental tests, the loading rate is kept approximately constant at 3 mm/min. The applied load is measured using a "Sewha, Korea" load cell five-ton capacity. Two LVDT have been used for measuring displacements of the models. Four strain gauges were attached to the piles while three strain gauges were attached to the raft. All of them were connected to a data logger with ten channels to measure the strain, two channels to measure the load, and two channels to measure the displacement. The data logger in turn was connected to a computer through an interface device to read the strain value.

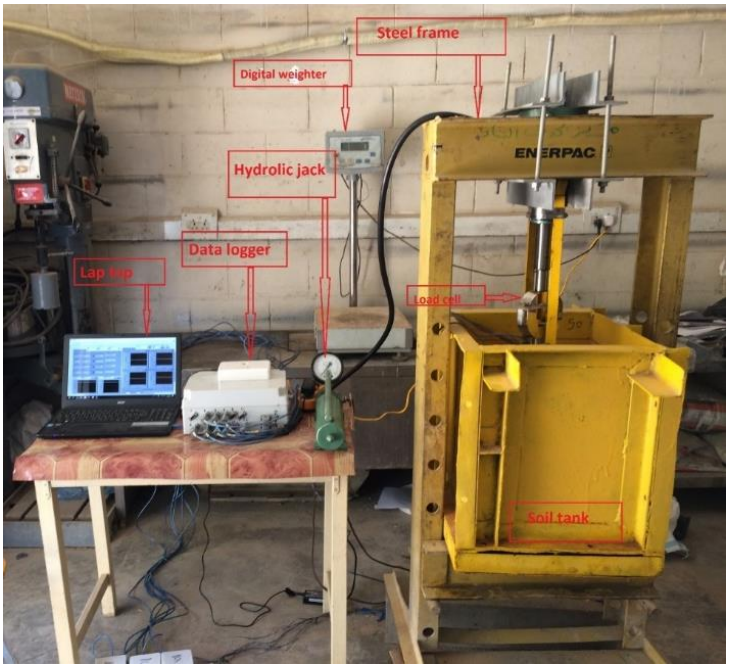

Figure 1. Testing system

The adopted soil tank has interior dimensions of 0.4 m length, 0.4 m width, and 0.5 m height. These dimensions are proposed to be compatible with test supporting frame. To have no interference between walls and the soil a clear distance of 142mm was provided from the face of the raft to the interior face of the wall tank. For the same purpose, a distance of two-times pile length was provided from the raft to the bottom of container as shown in Figure 2.

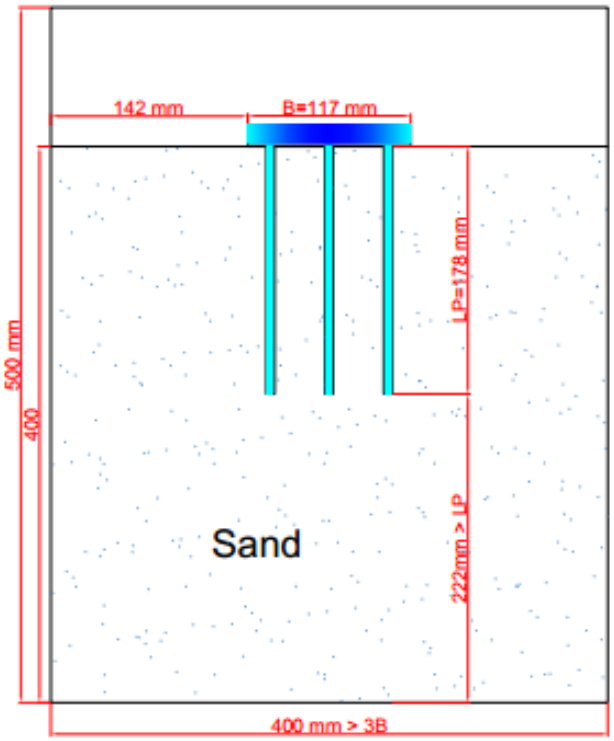

Figure 2. Soil tank with boundary condition

4. Soil Properties

The soil used for the model tests is clean, oven-dried, uniform quartz (Kerbela) sand. The maximum and minimum dry unit weights of the sand were determined according to the ASTM (D4253) and ASTM (D4254) specifications, respectively, the specific gravity test is performed according to ASTM (D854), the grain size distribution is analyzed according to ASTM (D422) specifications and direct shear test according to the ASTM (D3080). Figure 3 shows the grain size distribution of the sand and Table 2 summarize the physical properties of the tested sand. The angle of internal friction is determined using the direct shear test, which was carried out for the sand. The height of the sand was divided into 4 layers of 100 mm by knowing the weight and the volume of the sand it was sure compacted to 60% relative density (D_r).

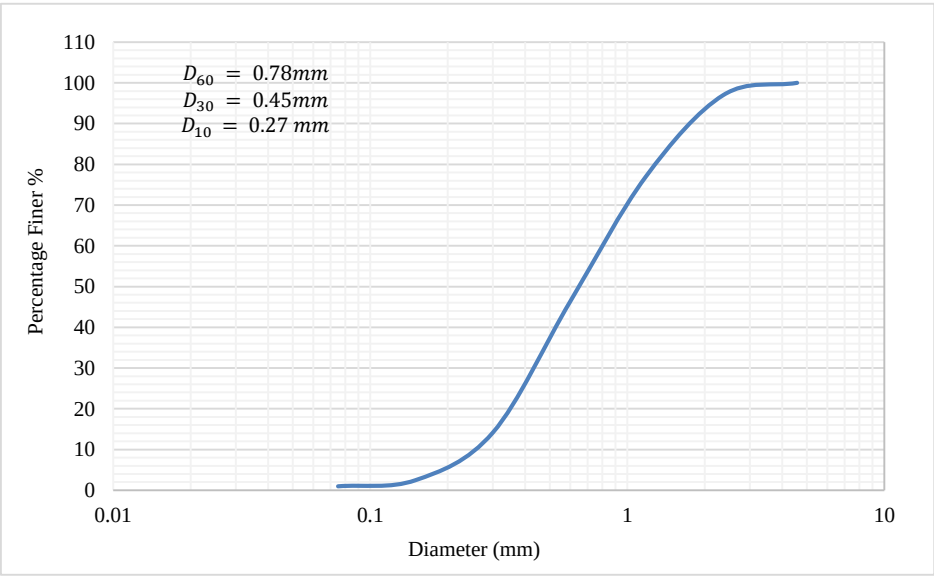

Figure 3. Grain size distribution of the sand

Table 2. Physical properties for the tested sand

Property	Value
Effective size, D_{10}	0.27
Coefficient of uniformity, C_u	2.89
Coefficient of curvature, C_c	0.96
Specific gravity, G_s	2.64
Maximum unit weight, γd_{max}	17.5 kN/m^3
Minimum unit weight, γd_{min}	14.3 kN/m^3
Test unit weight, γd_{test}	16.06 (kN/m^3)
Relative density, D_r	60%
Angle of friction φ	40

5. Strain Measurement

This experiment work adopts plastic strain gauges type GFLA-3-50-3LJC from TML, with the following characteristics: wire-type with a resistance of 120 Ω, a gauge factor of 2.09 +/- 1%, a gauge length of 3mm and width of 2.5mm.

Four strain gauges were attached to the PVC mini-piles, as indicated in Figure 4, to measure the strains at every load increment in the following locations:

- At the top and bottom of a corner mini-pile;
- At the top and bottom of the center mini-pile.

The strain gauge was covered with a layer of SB TABE size of 10mm width and 3mm thick to protect it from damage.

Figure 4. Strain gauges at corner and center piles with SB TABE

As indicated in Figures 5 to 6, three strain gauges were attached to the PVC raft as at the following locations to measure the strains:

- At an edge on the top surface;
- At the corresponding edge on the bottom surface;
- Near the center of the top surface.

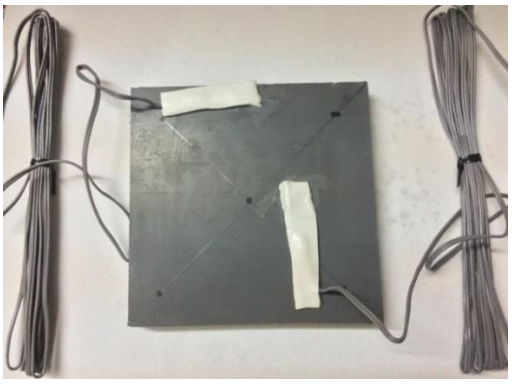

Figure 5. Strain gauges installation at the top raft

Figure 6. Strain gauge installation at the Bottom raft

6. Testing Procedure

The procedure followed in testing of the mini-piled raft models can be described in the following steps:

6.1. Building the Mini-piled Raft Foundation Model

PVC mini-piles have been grouped as indicated in Figure 7. Each pile has diameter of 6 mm and length of 178 mm. Notations adopted in the experimental work and in the subsequent discussion of the results have been summarized in Table 3 and Figure 7.

Table 3. Models Tests Program

Studied cases	Test Notations
Single mini-pile	MP
Raft thickness 15mm	R_{15}
Raft thickness 15mm with five mini-piles	MPR_{15}
Raft thickness 10mm with five mini-piles	MPR_{10}
Raft thickness 8mm with five mini-piles	MPR_{8}

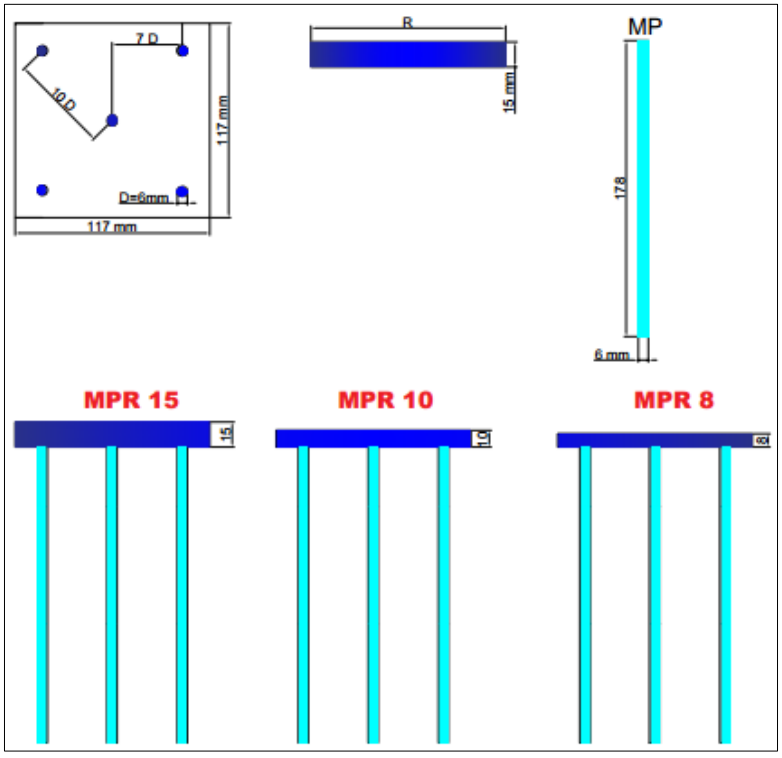

Figure 7. Case Studies

As indicated in Figure 8, the mini-piles were attached to the raft using a super glue to simulate a semi-fixed connection condition.

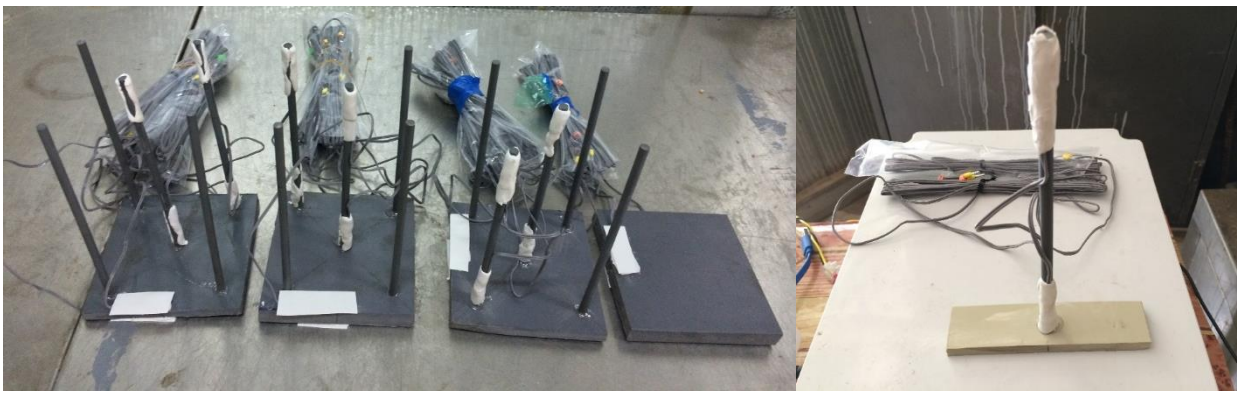

(a) Mini-piled raft and the raft models **(b) Single mini-pile model**

Figure 8. The MPR15, MPR10, MPR8, R, and MP models

6.2. Preparation of Sand Deposit and Placing of Mini-Piled Raft Model

The sand was placed in the tank with four layers, each layer of 100 mm thick and has a compacted relative density, D_r, of 60%. After each test, the tank should be emptied from the sand. During the sand filling process, the piled-raft model was placed at the center of the tank, then the sand was filled up to the bottom surface of the raft as presented in Figure 9.

Figure 9. The mini-piled raft model was placed in sand

6.3. Application of the Vertical Load

A concentrated vertical load is applied through a five-ton load cell at a constant loading rate. For each load increment, a sufficient time was given to full development of the corresponding strains and deformation. After each step, the load and the settlement were read the data logger through the corresponding channels. All gathered information have been saved in an Excel file. At end of the test, the sand was removed and the model was lifted.

7. Results and Discussion

7.1. Load Displacement Curves

Results for the load-displacement curves of the mini-piled raft foundation models are presented in Figures 10 to 14. Each figure contains two displacements from the attached two LVDTs. The average reading has been determined and presented also. Comparing between the two LVDT readings and their average value indicates that all foundations have uniform settlement during the loading process.

The load-displacement curves show that there is a 45% decrease in settlement for MPR15 comparing with R15, moreover there is no significant difference in settlement between MPR15, MPR10 and MPR8, where there is 1.5% difference between MPR15 and MPR10 and 7.8% between MPR15 and MPR8. This indicates that the considered different raft thicknesses have no significant effect on the geotechnical aspect of settlement reduction.

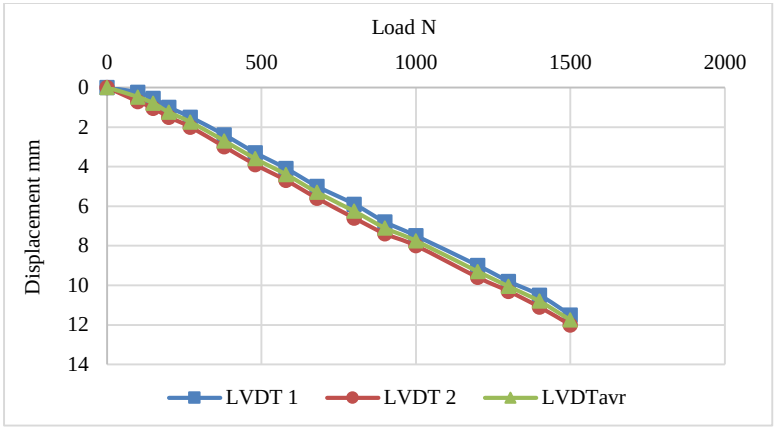

Figure 10. Load displacement curve for the raft R

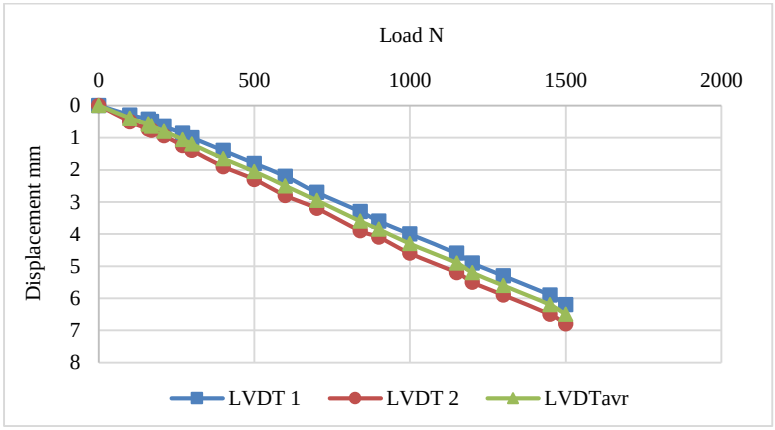

Figure 11. Load displacement curve for MPR15

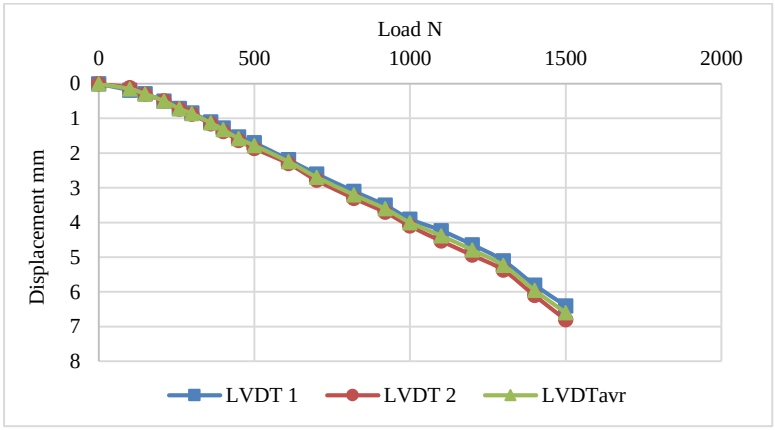

Figure 12. Load displacement curve for the MPR10

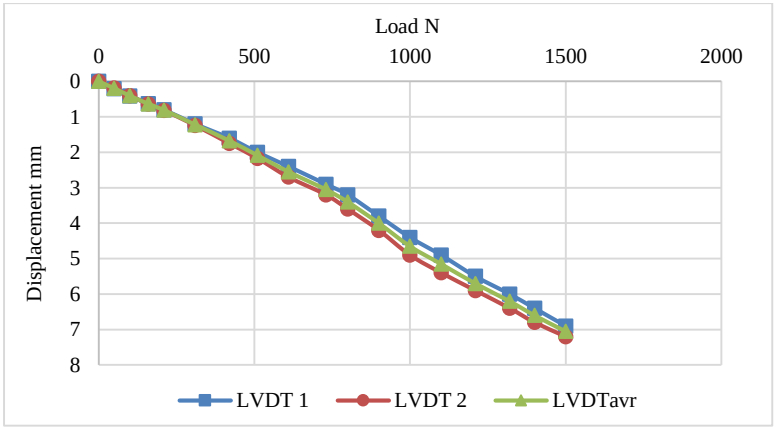

Figure 13. Load displacement curve for the MPR8

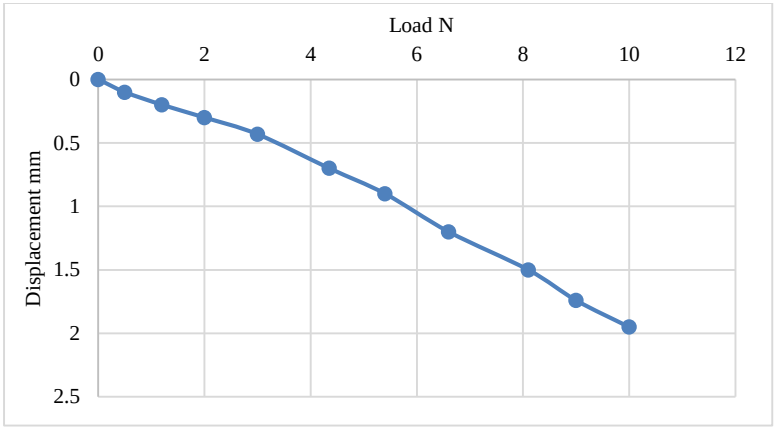

Figure 14. Load displacement curve for the MP

7.2. Bending Moment in the Rafts

The raft strain obtained from the test was used to calculate the moment M. Comparing the bending moments at the mid and edge of the mini-piled raft cases with those of the raft case indicates that the mini-piles significantly influence the structural behavior of the foundation.

Figure 15 presents the ratio between the bending moment at the mid of the mini-piled raft MPR15 to the corresponding bending moment at the raft R. It shows that the presence of the mini-piles decreases the bending moment ratio from 1 to 0.75 at the initial load and from 1 to 0.317 at the final load to indicate that there is a significant reduction, about 31.7%, in the moment at center of the mini-piled raft foundation compared with the corresponding moment of the control raft R. It is worthwhile to mention that the mini-piles have more significant role at the final loading stages comparing the initial loading stages.

Figure 16 presents the ratio between the bending moments at the mid of the mini-piled raft for different raft thicknesses to the bending moment of MPR15. This figure shows that the bending moment increases as the raft thickness decreases where it increases from 1 to 8.2, 4.9 in MPR10 and to 14.1, 10.8 in MPR8 at initial and final load respectively. These results indicate that the raft thickness has a significant effect on the moment distribution where a larger thickness leads to a more uniform distribution of moments that in turn reduce the maximum moment in the foundation.

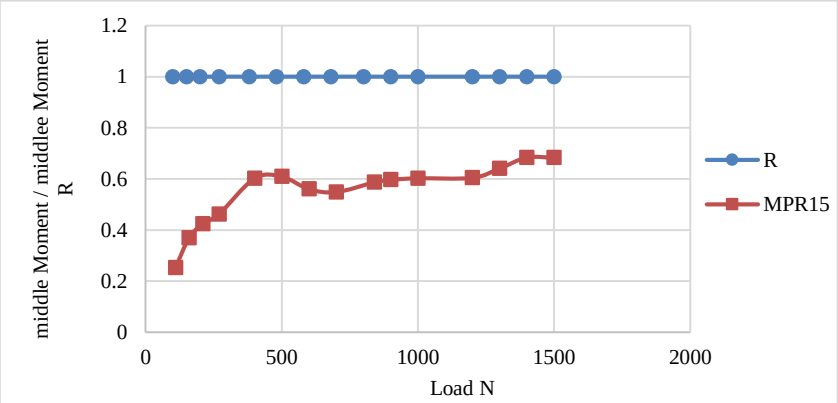

Figure 15. Bending moment at mid raft for R and MPR15

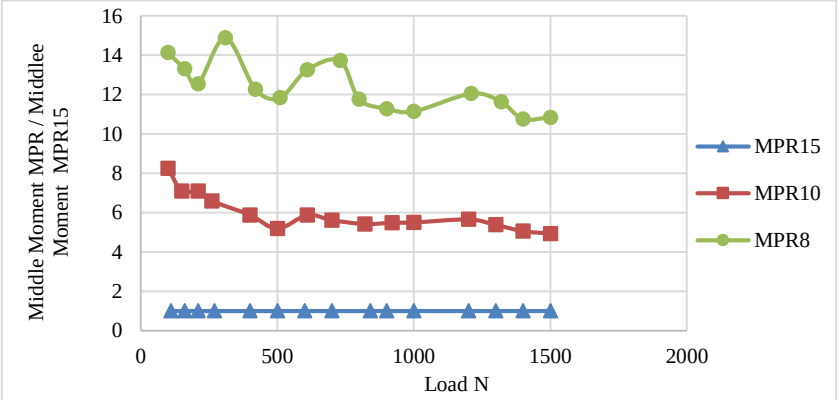

Figure 16. Bending moment at mid rafts for MPR

Figure 17 presents the ratio between the bending moments at the edge of the mini-piled raft MPR15 to the corresponding bending moment at the raft R. It shows that the presence of the mini-piles decreases the bending moment ratio from 1 to 0.74 at the initial load and from 1 to 0.8 at the final load, in other words, there is 20% reduction in the edge moment due to using of the mini-piles with raft foundation has a large thickness.

Finally, Figure 18 presents the bending moments ratios at the edge of the mini-piled raft for different raft thicknesses. As indicated in this figure, the bending moment at the edge increases as the raft thickness decreases. It increases from 1 to 3.68, 3 in MPR10 and to 11.2, 9.7 in MPR8 at initial and final load respectively. This can be explained in terms of thickness role where a larger thickness leads to a more uniform distribution of the moment and in turn to a reduction in the maximum moment value.

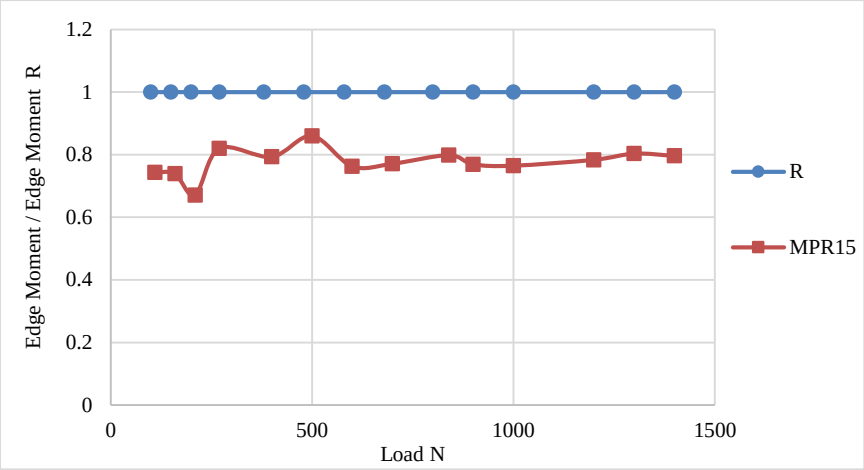

Figure 17. Bending moment at edge raft for R and MPR15

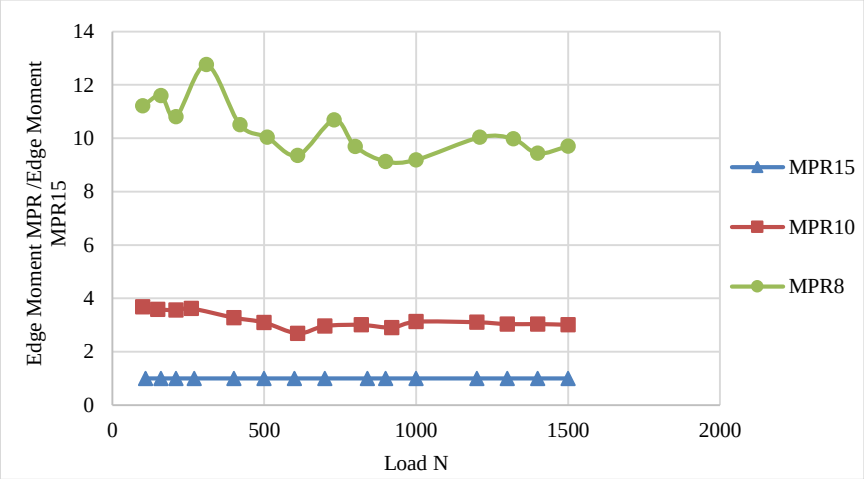

Figure 18. Bending moment at edge rafts for MPR

7.3. Axial Load in Top and Bottom Mini-Piles

The strain of the mini-piles obtained from the test was used to calculate the axial load, P, at the top and bottom of the mini-pile as indicated in Equation 3:

$$P = \varepsilon EA \tag{3}$$

Where A is the cross-section area of the mini-pile, ε is the axial strain measured from the strain gage, and E is the elastic modulus of PVC. Curves for the top and bottom axial load of the mini-piles at each load increment are presented in Figures 19 to 25. These figures illustrate that the axial load in the central mini-pile is higher than the axial load in corner mini-pile for all models. This trend of the results seems natural as the load is applied at the center of the raft and it acts directly on the central mini-pile. It is also observed that the axial load for the central and the corner mini-piles increases as the raft thickness decreases to indicate that mini-piles are more effective with thin models.

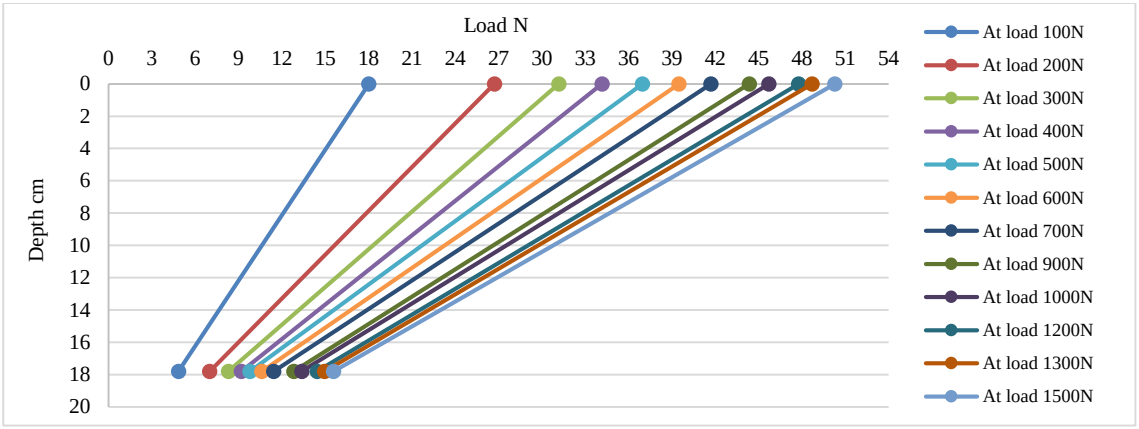

Figure 19. Load-depth curve for center mini-pile MPR15

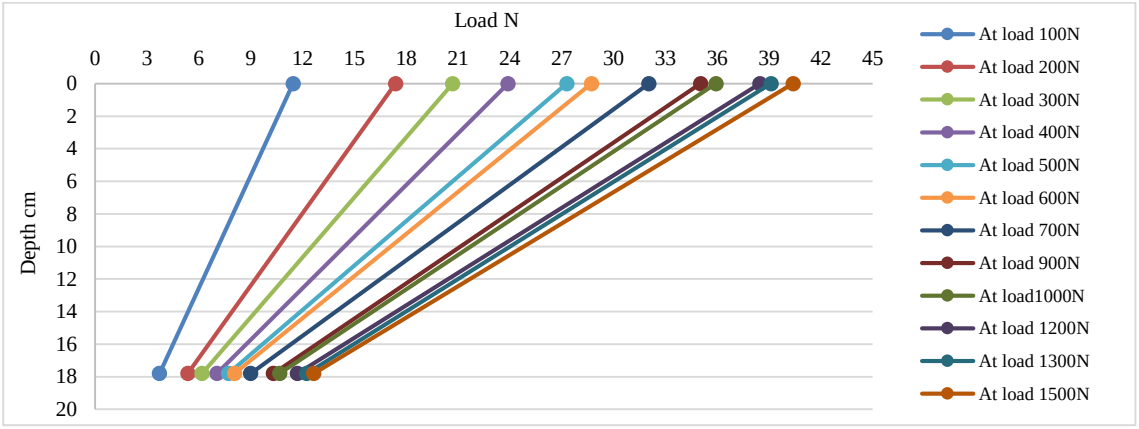

Figure 20. Load-depth curve for corner mini-pile MPR15

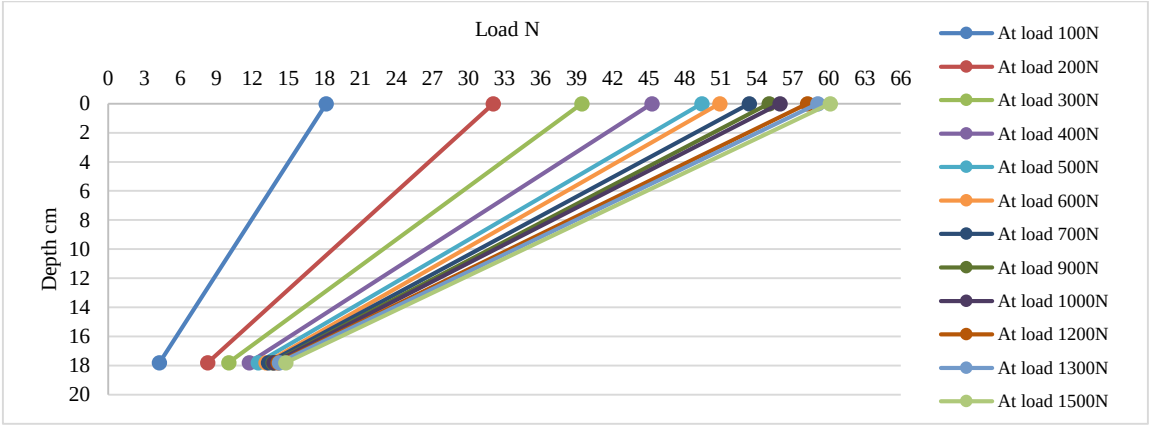

Figure 21. Load-depth curve for center mini-pile MPR10

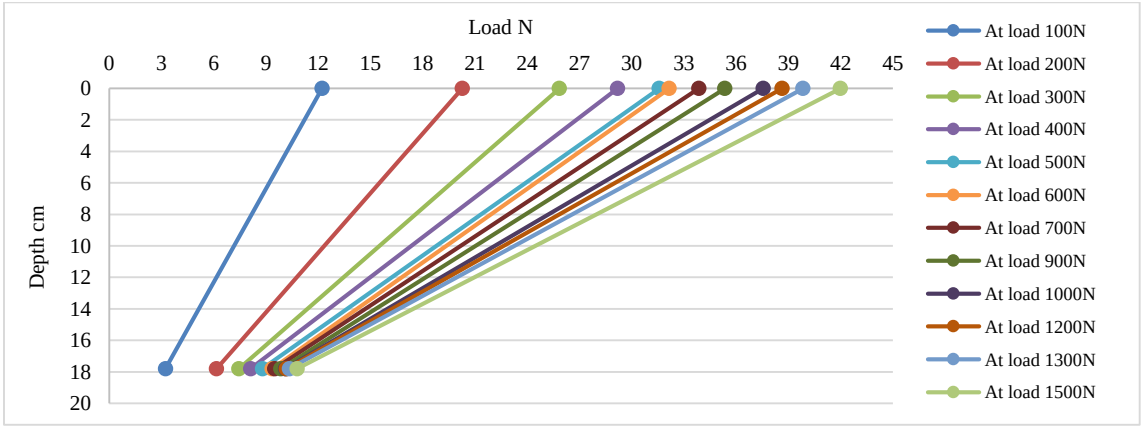

Figure 22. Load-depth curve for corner mini-pile MPR10

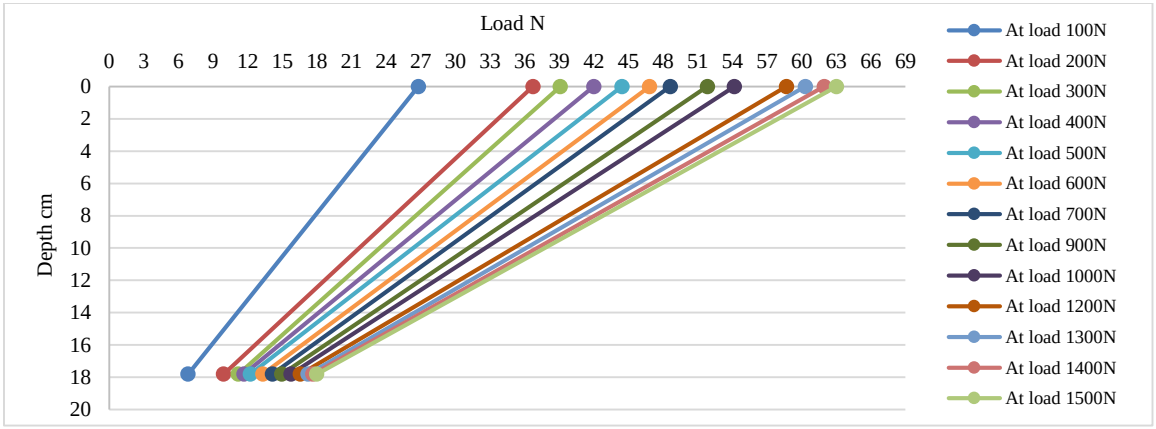

Figure 23. Load-depth curve for center mini-pile MPR8

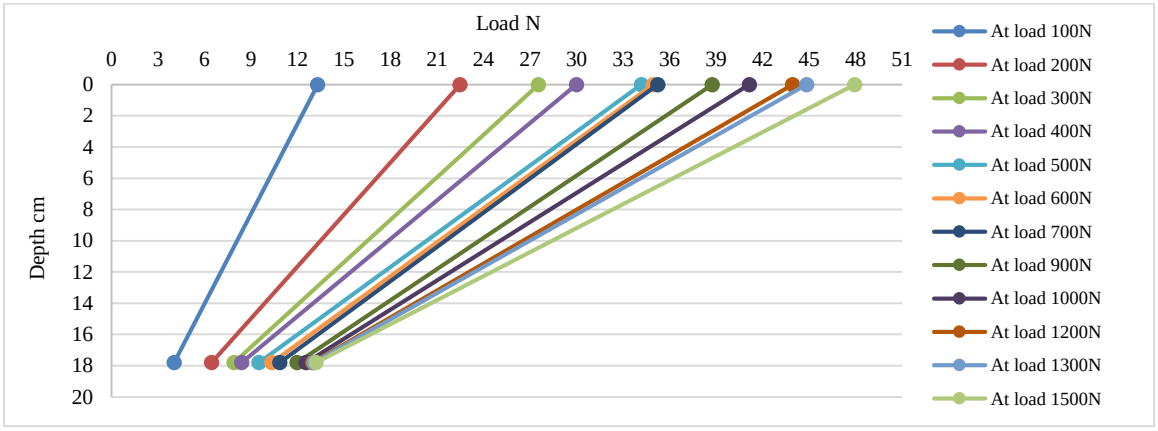

Figure 24. Load - depth curve for corner mini-pile MPR8

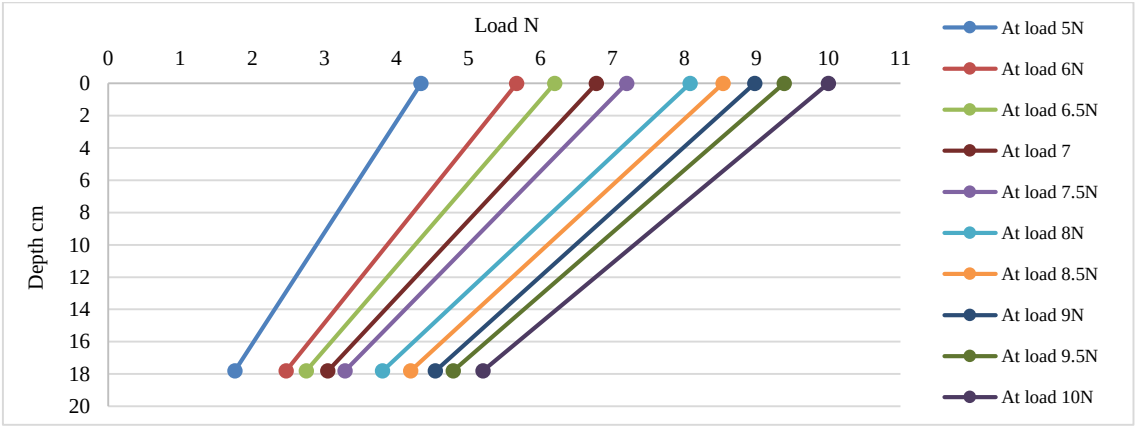

Figure 25. Load - depth curve for mini-pile MP

The friction for the mini-piles was calculated from Equation 4 and it has been presented in percentage form as indicated in Table 4 below. This table shows that most of the mini-pile axial loads are transferred to the underneath soil through friction and that the friction for the central and corner mini-piles increases as the raft thickness decreases.

$$friction = P_{top} - P_{bottom} \quad (4)$$

Table 4. Percentage of the friction to the total pile load at initial and final loading

Mini-pile	Percentage of friction at the initial loading (%)	Percentage of friction at the final loading (%)
Center mini-pile MPR15	73	69
Corner mini-pile MPR15	68	69
Center mini-pile MPR10	75	73
Corner mini-pile MPR10	71	72
Center mini-pile MPR8	76	74
Corner mini-pile MPR8	72	73
Single mini-pile	57	47

7.4. Load Carried by Mini-Piles or Raft

Comparison of load carried by the mini-pile and the raft are presented in curves of Figures 26 to 28. At the initial loading stage, most of the load is carried by the mini piles due to reduction of the contact between the raft and underneath soil. As the applied load increases, the proportion of the load carried by the piles gradually decreases. At load of 0.8 kN approximately, the load transferred by the mini-piles becomes almost constant. At final stage, the loads carried by the rafts for the MPR8, MPR10, and MPR15 foundations respectively were 83%, 85% and 86% of the total applied loads.

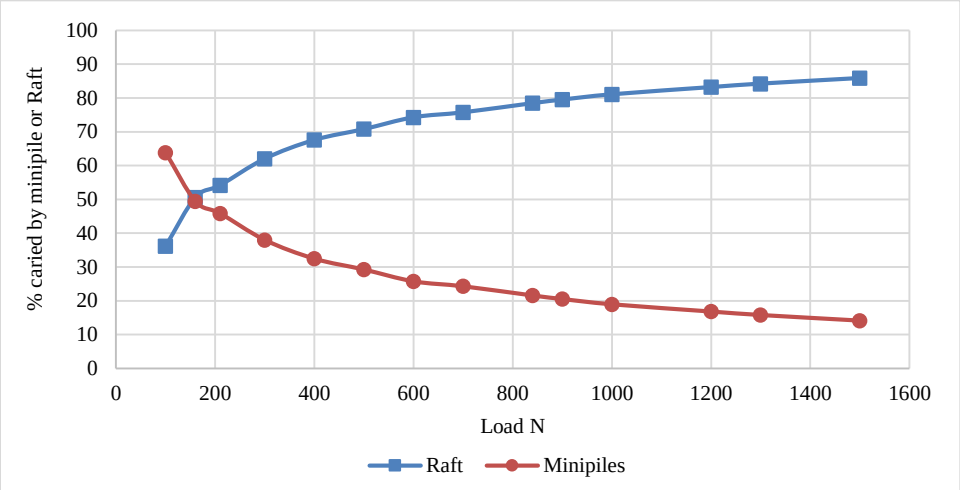

Figure 26. Percentage of load carried by mini-piles or raft curve for MPR15

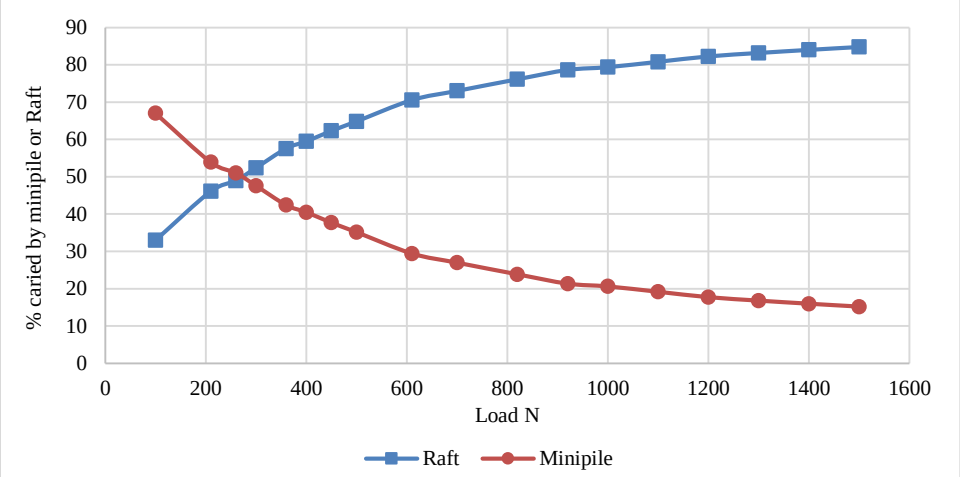

Figure 27. Percentage of load carried by mini-piles or raft curve for MPR10

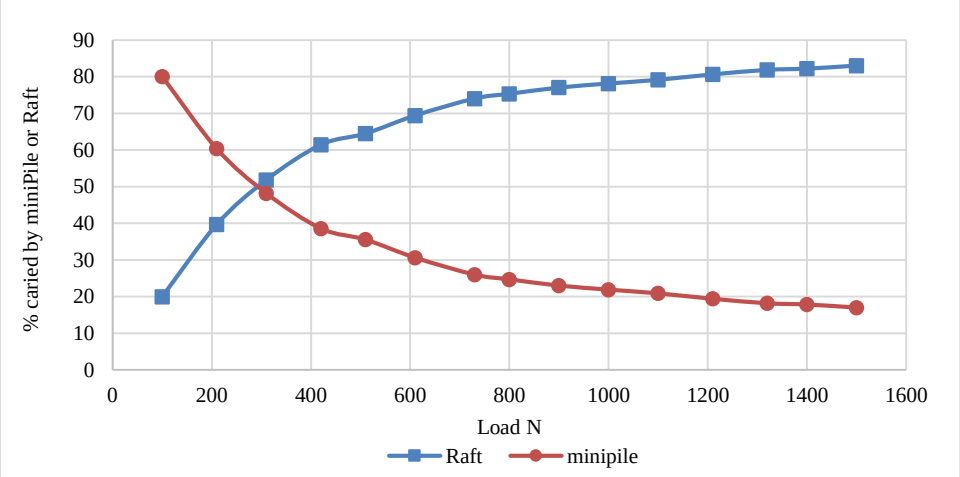

Figure 28. Percentage of load carried by mini-piles or raft curve for MPR8

8. Conclusions

Five tests were conducted to investigate the behavior of mini-piled raft foundations, with a varying raft thickness, in a dry sandy soil under a concentrated vertical load. The following conclusions may be pointed:

- There is a 45% decrease in settlement for 15mm mini-piled raft foundation comparing with the reference 15mm raft foundation. Moreover, there is no significant difference in settlement between 15mm mini-piled raft foundation comparing with the 10mm and 8mm thick mini-piled raft foundations.
- The bending moment decreases at the mid and edge of the 15mm mini-piled raft foundation comparing to those of the reference raft foundation. It has also been noted that the moments are inversely proportional to the thickness of the piled raft foundations.
- With respect to the mini-piles, it has been found that most of the pile axial loads are transferred to the underneath soil through friction and this friction increases as the raft thickness decreases.
- The loads carried by the rafts for the 8mm,10 mm,15 mm thick mini-piled raft foundations respectively were 83%, 85% and 86% of the total applied loads.

9. Funding

This work supported by the laboratories of Building Research Directorate, Ministry of Construction Housing and Municipalities, Baghdad, Iraq.

10. Conflict of Interest

The authors declare no conflict of interest.

11. References

[1] FHWA "Micropile Design and Construction: Reference Manual," Washington, D.C.: U.S. Department of Transportation, 2005.

[2] Bruce, D., & Juran, L. "Drilled and Grouted Micropiles: State-of-Practice Review," Virginia: U.S. Department of Transportation, Federal Highway, 1997.

[3] Barron, D. "Finite Element Modeling Of Micropiles And The Influence Of Steel Casing On Load Transfer Mechanisms," ProQuest LLC, New York, 2016.

[4] Jeon, S., & Kulhawy, F. "Evaluation of Axial Compression Behaviour of Micropiles," Proceedings of a specialty conference: Foundations and Ground Improvement, Blacksburg, Virginia, 2001.

[5] Tsukada, Yukihiro, Kinya Miura, Yukitomo Tsubokawa, Yoshinori Otani, And Guan-Lin You. "Mechanism of Bearing Capacity of Spread Footings Reinforced with Micropiles." Soils and Foundations 46, no. 3 (2006): 367–376. doi:10.3208/sandf.46.367.

[6] Kyung, Doohyun, Daehong Kim, Garam Kim, and Junhwan Lee. "Vertical Load-Carrying Behavior and Design Models for Micropiles Considering Foundation Configuration Conditions." Canadian Geotechnical Journal 54, no. 2 (February 2017): 234–247. doi:10.1139/cgj-2015-0472.

[7] Hwang, Tae-Hyun, Kang-Hyun Kim, and Jong-Ho Shin. "Effective Installation of Micropiles to Enhance Bearing Capacity of Micropiled Raft." Soils and Foundations 57, no. 1 (February 2017): 36–49. doi:10.1016/j.sandf.2017.01.003.

[8] Sharma, Binu, Sushanta Sarkar, and Zakir Hussain. "A Study of Parameters Influencing Efficiency of Micropile Groups." Ground Improvement Techniques and Geosynthetics (September 2, 2018): 11–18. doi:10.1007/978-981-13-0559-7_2.

[9] Alnuaim, A.M., H. El Naggar, and M.H. El Naggar. "Performance of Micropiled Raft in Sand Subjected to Vertical Concentrated Load: Centrifuge Modeling." Canadian Geotechnical Journal 52, no. 1 (January 2015): 33–45. doi:10.1139/cgj-2014-0001.

[10] Rose, A.V., R.N. Taylor, and M.H. El Naggar. "Numerical Modelling of Perimeter Pile Groups in Clay." Canadian Geotechnical Journal 50, no. 3 (March 2013): 250–258. doi:10.1139/cgj-2012-0194.

[11] Alnuaim, Ahmed M., M. Hesham El Naggar, and Hany El Naggar. "Numerical Investigation of the Performance of Micropiled Rafts in Sand." Computers and Geotechnics 77 (July 2016): 91–105. doi:10.1016/j.compgeo.2016.04.002.

[12] ZOLFEGHARIFAR[1], Sayyed Yaghoub, Hadi DARAM[1], and Majid RAHIMI[1]. "Static Analysis, Using Finite-Element Method (FEM) for Micropiles Application Evaluation: Empirical and Numerical Perspective." Fen Bilimleri Dergisi (CFD) 36, no. 4 (2015).

[13] El Sharnouby, M. M., and M. H. El Naggar. "Numerical Investigation of Axial Monotonic Performance of Reinforced Helical Pulldown Micropiles." International Journal of Geomechanics 18, no. 10 (October 2018): 04018116. doi:10.1061/(asce)gm.1943-5622.0001161.

[14] Poulos, H. G., & Davis, E. H. "Elastic Solutions for Soil and Rock Mechanics", New York: John Wiley and Sons. Inc, 1974.

[15] Randolph, M. F. "Design Methods for Piled Groups and Piled Rafts.," In Proceedings of the 13th international conference on soil mechanics and foundation engineering, no. New Delhi, India., pp. 61-82, 1994.

[16] Poulos, H. G. "Piled Raft Foundations: Design and Applications." Géotechnique 51, no. 2 (March 2001): 95–113. doi:10.1680/geot.2001.51.2.95.

[17] Tuan. "A Simplified Formular for Analysis Group Efficiency of Piles in Granular Soil," International Journal of Scientific & Engineering Research, p. 7(7), 2016.

[18] Xu, Ling-Yu, Jing-Min Pan, Ying-Ying Xue, and Fei Cai. "A Numerical Investigation of Influence of Low-Plasticity Fines in Sand on Lateral Response of Piles." Marine Georesources & Geotechnology (February 22, 2019): 1–10. doi:10.1080/1064119x.2019.1569740.

[19] A. Mahboubi and A. Nazari-Mehr. "Nonlinear Dynamic Soil-Micropile-Structure Interactions Centrifuge Tests and FEM Analyse," In Proceeding of the Deep Foundations and Geotechnical In Situ Testing, GeoShanghai 2010 , China, 2010.

[20] Richards, T. D., & Rothbauer, M. J. "M.J. 2004. Lateral Loads on Pin Piles (Micropiles)," InProceedings of the GeoSupport Conference: Innovation and Cooperation in the GeoIndustry Orlando, no. Florida, pp. 158-174, 2004.

[21] Shahrour, I., and N. Ata. "Analysis of the Consolidation of Laterally Loaded Micropiles." Proceedings of the Institution of Civil Engineers - Ground Improvement 6, no. 1 (January 2002): 39–46. doi:10.1680/grim.2002.6.1.39.

[22] Teerawut, J. "Effect of diameter on the behavior of laterally loaded piles in weakly cemented sand," Ph.D. Dissertation, University of California, San Diego, California, 2002.

[23] Kershaw, Kyle, and Ronaldo Luna. "Scale Model Investigation of the Effect of Vertical Load on the Lateral Response of Micropiles in Sand." DFI Journal - The Journal of the Deep Foundations Institute 12, no. 1 (January 2, 2018): 3–15. doi:10.1080/19375247.2018.1462040.

[24] Wood, D. M. "Geotechnical Modelling," 1st ed. CRC Press, Boca Raton, FL, 2004.